

## MOMENT-CURVATURE DIAGRAMS FOR EVALUATION OF SECOND ORDER EFFECTS IN RC ELEMENTS

H. Barros<sup>1</sup>, C. Ferreira<sup>1</sup>, and T. Marques<sup>2</sup>

<sup>1</sup> INESCC – Department of Civil Engineering, University of Coimbra

Rua Luís Reis Santos - Pólo II da Universidade, 3030-788 Coimbra, Portugal  
{hbarros,Carla}@dec.uc.pt

<sup>2</sup> COBA, Consultores de Engenharia e Ambiente, S.A. Av. 5 de Outubro, 323, 1649-011 Lisboa

**Keywords:** Reinforced concrete, moment-curvature, stiffness, EC2, beam deflection.

**Abstract.** *The analytical ( $M-1/\rho$ ) relationship is obtained with Mapple software considering the static equilibrium equations (of bending moment  $M$  and axial load  $N$ ) and compatibility of deformations (between steel and concrete) at the section level [1]. The present work uses a closed form of the relation ( $1/\rho-M$ ) with the Ramberg and Osgood equation [2], representing in a unique way the stages of: cracked concrete with steel in elastic range and cracked concrete with steel in the plastic range. To consider uncracked concrete in the global member behaviour the model of the European code [3] is used. The numerical results consist of moment curvature diagrams of reinforced concrete sections and load – deflection curves of reinforced concrete beams.*

## 1 INTRODUCTION

In structures composed of linear elements where one dimension is more significant than the others, such as beams and columns, a relation can be derived between the bending moment  $M$  and the curvature ( $1/\rho$ ) at the section level, and the deformation produced by the tangential stresses disregarded. This moment ( $M$ ) - curvature ( $1/\rho$ ) relation takes the form of a differential equation for the transverse displacement of the structural member in an homogeneous material.

In composite beams made of materials with different behaviour in tension and compression, such as concrete, and steel reinforcement, the ( $M$ ) - curvature ( $1/\rho$ ) relation varies with the section along the structure. Several models to predict the global behaviour of these structures are used and described next.

Many ( $M - 1/\rho$ ) equations are known such as the trilinear relationship, presented by Zheng et al [4], to predict flexural sectional response of beams with reinforced polymer rebars.

In the work of Torrico [5] the linearization of the moment vs curvature is used to obtain the pos-critical behaviour of high strength reinforced concrete (RC) columns, taking into account the geometrical and material nonlinearities including the confining effect of the transversal reinforcement. The values obtained are compared to experimental results of columns with different slenderness and reinforcement ratios.

The use of a moment-curvature law modelling the material softening due to cracking in reinforced concrete beams is made in Challamel et al [6]. Ponaya et al [7] uses this law to represent, in a simplified unidimensional approach, the local buckling phenomenon in steel thin-walled structures.

In Picandet et al [8] the moment-curvature relation is also used to model the geometrical softening due to the global instability in compressed columns. In this paper, a bilinear moment-curvature relation is considered with a first branch representing the elastic behaviour and a second branch the inelastic. Three alternatives in the inelastic branch are available: hardening, softening and perfect plastic. All of them are considered in the development of the analytical solution of the differential equation governing the lateral deflection of the column, clamped at the base and free at the top, where an axial load is applied. Load-deflection diagrams [8] are obtained considering simultaneously geometric and material non-linearities.

In Casandjian et al [9], the moment curvature relation at the section level is obtained using tension- deformation constitutive laws.

In the work of Caglar et al [10], the moment curvature diagrams are used to obtain the flexural stiffness of reinforced concrete columns with circular cross section, to be used in genetic programming with artificial intelligence. This technique is also applied by Cevik et al [11] and Chen et al [12].

According to European codes [3,13], the tension stiffening effect, due to the contribution of the concrete between cracks to the global behaviour, can be considered by two different ways: approaching the average strain (or curvature or stiffness) or using an effective area of concrete, which is equivalent to consider a mean modulus of elasticity. Both procedures use the concept of average constitutive laws of cracked concrete and reinforcing steel and are present in Vecchio et al [15] and Vecchio [16].

Kwak et al [17] use the average strain concept, considering the contribution of fully cracked and uncracked concrete and also a model to approach the bond-stresses between steel and surrounding concrete.

Kaklauskas et al [18] use the moment-curvature diagrams of RC beams obtained with ATENA software in a nonlinear finite element analysis, dividing the cross section into layers with perfect bond between them.

Márquez et al in [19] analyse the moment-curvature relations of concrete piles, with circular cross sections and different arrangement of reinforcement, such as the symmetric and the asymmetric, and compare them to Eurocode 2 [3] and CEB-fib Model Code 2010 [20] proposed expressions.

In the present paper the analytical ( $M - 1/\rho$ ) formulation takes into account concrete cracking under tension, linear elastic law in compression and steel with either elastic or plastic behaviours. Considering all these aspects the ( $M - 1/\rho$ ) relation becomes nonlinear. The identified three stages are: a) uncracked concrete; b) cracked concrete and steel in the elastic domain and c) cracked concrete and steel in the plastic domain. The end of stage c) corresponds to the ultimate design, solved for multi-rectangular concrete sections in [14]. In this paper an approximation with Ramberg and Osgood equation of the inverse relation, that is the curvature ( $1/\rho$ ) as a function of the moment ( $M$ ), is made. This procedure delivers a unique equation of the two concrete cracked stages within the section level, representing the behaviour of cracked sections. In order to obtain the global behaviour of the cracked member, both cracked and uncracked zones must be considered (usually named tension softening effect). The average curvature [3] is used in the present work.

The examples presented show the application of the developed model to obtain the moment-curvature of a reinforced concrete sections and the load deflection of reinforced concrete beams. The results are in good agreement with experimental and analytical results of other authors.

## 2 REINFORCED CONCRETE MEMBER BEHAVIOUR

The overall behaviour of the reinforced concrete member is ruled by the uncracked and cracked zones. The basic assumptions for singly reinforced concrete rectangular cross sections, defined by the width  $b$ , height  $h$ , concrete cover  $a$  (distance between steel centroid and concrete border), steel tension area  $A_s$  and steel compression area  $A'_s$  (see Fig. 1), are described in the next sections.

### 2.1 Basic assumptions

The fundamental assumptions of the behaviour of flexural beams are [3]:

- the cross section remains plane after the deformation, see Fig.1;
- full adherence between concrete and steel;
- the concrete stress-strain constitutive law is linear elastic in compression and in tension, with elasticity modulus  $E_c$ ; in tension the maximum stress in concrete is  $f_{ctm}$ ; when the tensile concrete stress attains  $f_{ctm}$  the section is considered cracked, and the global behaviour of the member depends on both cracked and uncracked sections;
- the steel stress-strain relation is linear elastic, with elasticity modulus  $E_s$ , up to the design yield stress  $f_{yd}$ . After this value a constant stress of  $f_{yd}$  is considered (plastic domain).

Considering the concrete linear elastic relation in compression is an approximation allowed in EC2 [3] for service loads, for stress less than  $0.4f_{cm}$  ( $f_{cm}$  is the mean compressive strength). As a matter of fact the existence of cracked sections influences more the beam deflection in service, than the simplification due to the linear relation in the compressed concrete. Usually, the structures ductility is an important issue in concrete design, meaning that their collapse

occurs with steel rebars  $A_s$  in the plastic domain. The possibility of the steel plastification is considered in the present model.

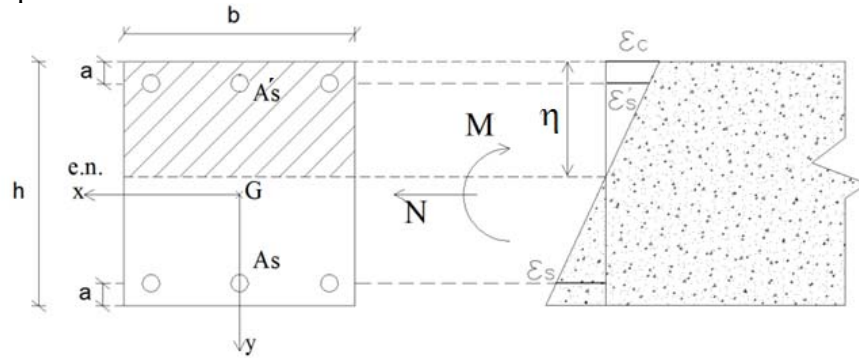


Figure 1: Geometrical definitions of the cross section and deformation.

## 2.2 Overall behaviour of the cracked member

The overall behaviour of the cracked member after the appearance of the first crack is divided into the zones: before the appearance of the first crack; formation of the cracks and the stabilized cracking, see Fig. 2a,b) [3]. In the figures state I is the  $(M - 1/\rho)$  evaluated in an uncracked section and State II<sub>0</sub> in a cracked section, both cases under pure bending. Under axial load and bending moment the curvatures are termed  $1/\rho_1$  and  $1/\rho_2$  in states I and II, respectively.

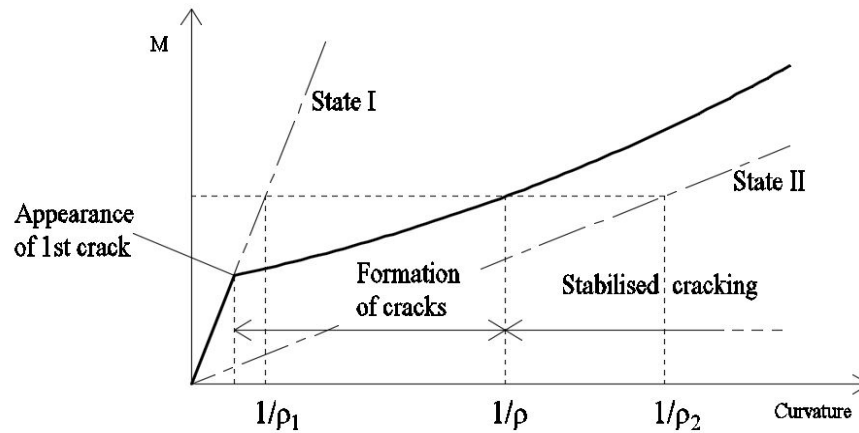


Figure 2a): Idealized moment curvature behaviour for bending moment [3].

In state I the curvature  $\frac{1}{\rho_1}$  for pure bending or bending moment and axial load is considered the same [3]. The curvature for state II, bending moment and axial load, can be related to the curvature in pure bending, by  $\frac{1}{\rho_2} = \frac{1}{\rho_{20}} + \frac{1}{\rho_{2N}}$ . The curvature  $\frac{1}{\rho_{2N}}$  is caused by the bending moment due to the axial force  $N$  acting at the centre of gravity of the total section in State I, being displaced from the centre of gravity of the cracked section.

The mean curvature  $\frac{1}{\rho}$ , that takes into account the contribution of the concrete between cracks, is given by, see [3]:

$$\frac{1}{\rho} = (1 - \zeta) \frac{1}{\rho_1} + \zeta \frac{1}{\rho_2} \quad (1)$$

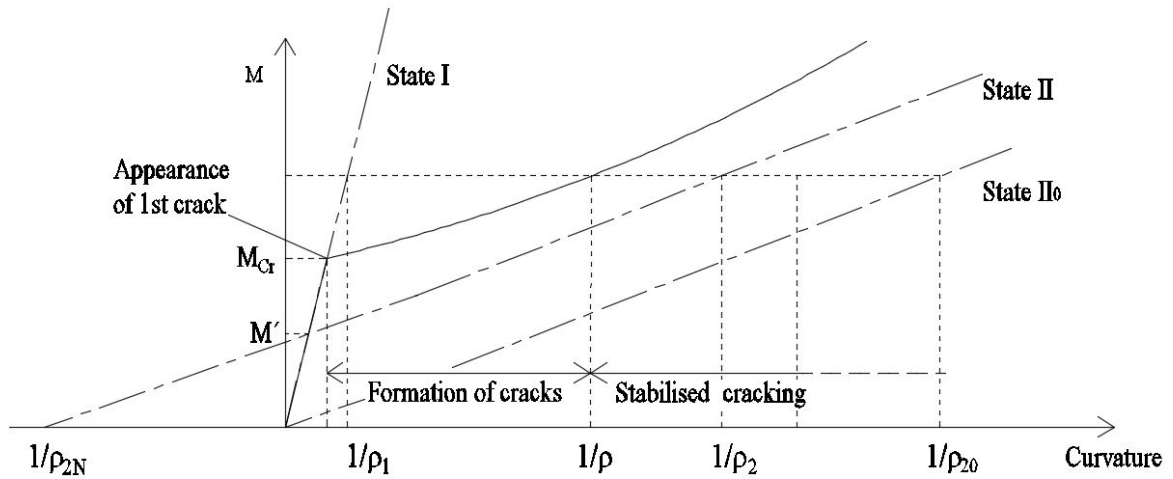


Figure 2b): Idealized moment curvature behaviour for bending moment and axial load [3].

The parameter  $\zeta$  in pure bending or with bending moment and axial load is a function of: the maximum moment before cracking,  $M_{cr}$ ; the resultant moment  $M$  at the centroid of the concrete section (middle height in the rectangular section); the adherence between steel and concrete defined by  $\beta$ . According to CEB Manual [13]  $\zeta$  is given by:

$$\zeta = 1 - \beta \left( \frac{M_{cr}}{M} \right)^2 \text{ if } N=0 \quad (2a)$$

$$\zeta = 1 - \left( \frac{\sqrt{\beta} M_{cr} - M'}{M - M'} \right)^2 \text{ if } N \neq 0 \text{ and } \sqrt{\beta} M_{cr} \geq M' \quad (2b)$$

$$\zeta = 1 \text{ if } N \neq 0 \text{ and } \sqrt{\beta} M_{cr} < M' \quad (2c)$$

The moment  $M'$  is the intersection of the moment curvature for state I and II, as represented in Fig. 2b).

### 2.3 Static equations

The static equations at the section reveal the axial load  $N$  by the integration of normal stresses in concrete  $\sigma_c$  and steel  $\sigma_{si}$ , and the bending moment  $M$  by a similar procedure, that is:

$$N = \int_{A_c} \sigma_c dA_c + \sum_{i=1}^n \sigma_{si} A_{si} \quad (3)$$

$$M = \int_{A_c} \sigma_c y dA_c + \sum_{i=1}^n \sigma_{si} y_i A_{si} \quad (4)$$

where:

$A$  – area of active concrete;

$\sigma_c, \sigma_{si}$ , – concrete, steel stress at  $Y_i$  coordinate;

$A_{si}$  – steel area;

$y_i$  and  $y$  – distances to the centroid (see Fig.1);

$G$  – centroid of the section

### 3 MOMENT CURVATURE EQUATIONS AT SECTION LEVEL

The assumptions exposed in 2.1 lead to three stages of the reinforced concrete section and corresponding equilibrium equations (3) and (4), that are:

- a) uncracked concrete with the steel in the elastic range;
- b) cracked concrete with the steel in the elastic range;
- c) cracked concrete with the steel in the plastic domain;

In each stage the procedure is the following:

- 1- compute the axial load  $N$ ;
- 2- the axial load value determines the neutral axis position  $\eta$ ;
- 3- the bending moment  $M^*$  that equilibrates the axial load is found at the neutral axis or at middle height  $M$ .

Section 3.1 presents the moment-curvature relation for uncracked reinforced concrete section. Section 3.2 resumes the expressions for  $N$ ,  $\chi$ ,  $M$  or  $M^*$  after concrete cracking. Using the methodology described in section 3.3 a moment-curvature relationship can be obtained. A closed form of the  $(1/\rho-M)$  relationship is derived by the use of Ramberg and Osgood equation and Goldberg Richard power representation, as presented in section 4.

Finally, the global behaviour of the member with the contribution of the stiffness due to the concrete between cracks is achieved.

#### 3.1 Uncracked concrete

Before concrete cracking, the steel is in the elastic domain and the section is homogenized in concrete through the factor  $\alpha = E_s/E_c$ , multiplying the steel area [3]. The moment  $M^*$  versus curvature  $1/\rho$  relation is given, in function of the neutral axis position,  $\eta$ , by:

$$M^* = \frac{1}{\rho} E_c \left[ I_c + bh \left( \frac{h}{2} - \eta \right)^2 + A_s \alpha (h - a - \eta)^2 + A'_s \alpha (a - \eta)^2 \right] \quad (5)$$

The neutral axis in the elastic domain is located at the centroid of the section, defined by the particular position  $\eta_G$ , given through the equation:

$$\eta_G = \frac{\frac{bh^2}{2} + A_s \alpha (h - a) + A'_s \alpha a}{bh + (A_s + A'_s) \alpha} \quad (6)$$

The maximum moment before cracking, termed  $M_{cr}$ , that is the moment for which the maximum tensile stress in concrete is equal to the mean value of the tensile strength,  $f_{ctm}$ , and the corresponding curvature  $(1/\rho)_{cr}$  are the following:

$$M_{cr} = \left[ f_{ctm} + \frac{N}{bh + (A_s + A'_s) \alpha} \right] \frac{EI}{(h - \eta_G) E_c}; \quad (1/\rho)_{cr} = \frac{M_{cr}}{EI} \quad (7)$$

With:

$$EI = E_c \left[ I_c + bh \left( \frac{h}{2} - \eta_G \right)^2 + A_s \alpha (h - a - \eta_G)^2 + A'_s \alpha (a - \eta_G)^2 \right] \quad (8)$$

and

$$I_c = \frac{bh^3}{12} \quad (9)$$

The parameter  $\zeta$  is computed by substituting the maximum moment before cracking,  $M_{cr}$ , into equation (2). The moment-curvature relation in the uncracked concrete, state I, is then written as follows:

$$\left[\frac{1}{\rho}\right]_1 = \frac{M}{EI} \quad (10)$$

### 3.2 Cracked concrete

In the reinforced concrete section, after the cracking of the concrete under tension, two stages are considered: the tension steel  $A_s$  in the elastic range or in the plastic. The compression steel  $A'_s$  and the concrete are considered elastic.

#### 3.2.1 Cracked concrete and steel in the elastic range

At the initial stage, when the steel is yet in the elastic range, the static equation (3) is rewritten:

$$N = \frac{\eta^2 b E_c}{2\rho} + \frac{A_s E_s}{\rho} (a - h + \eta) + \frac{A'_s E_s}{\rho} (\eta - a) \quad (11)$$

Solving equation (11) in terms of  $\eta$ , the neutral axis position is given by:

$$\eta = \left[ -\frac{(A_s + A'_s)\alpha}{b} + \left( \frac{\alpha^2 (A_s + A'_s)^2}{b^2} + \frac{2}{b} \left( \frac{\rho N}{E_c} + \alpha A_s (h - a) + \alpha A'_s \right) \right)^{1/2} \right] \quad (12)$$

Equation (4) then becomes:

$$M^* = \frac{\eta^3}{3\rho} b E_c + \frac{(a - h + \eta)^2}{\rho} E_s A_s + \frac{(\eta - a)^2}{\rho} E_s A'_s \quad (13)$$

#### 3.2.2 Cracked concrete and steel in the plastic range

After the concrete cracking but with steel  $A_s$  in the plastic range, that is the stress equal to  $f_{yd}$ , equations (11, 12 and 13) become:

$$N = \frac{1}{2\rho} \eta^2 b E_c - A_s f_{yd} + \frac{1}{\rho} (\eta - a) E_s A'_s \quad (14)$$

$$\eta = -\frac{\alpha A'_s}{b} + \left[ \left( \frac{\alpha A'_s}{b} \right)^2 + \frac{2\rho}{b E_c} \left( \frac{a E_s A'_s}{\rho} + N + A_s f_{yd} \right) \right]^{1/2} \quad (15)$$

$$M^* = \frac{E_c b \eta^3}{3\rho} - A_s f_{yd} (a - h + \eta) + \frac{1}{\rho} (\eta - a)^2 E_s A'_s \quad (16)$$

The bending moment evaluated at the centroid of the concrete section (middle height) is:

$$M = M^* + N \left( \frac{h}{2} - \eta \right) \quad (17)$$

The equations (11) to (17) lead to the representation in Fig. 3 for a particular section and material properties (defined in the numerical results) and variable axial load ( $N = 0; 100; 500; 1000 \text{ kN}$ ), denoting that  $1/\rho = \eta/(h - a)$ . In Fig. 3 the elastic range both in

concrete and steel is not represented and the curves are truncated for the curvature corresponding to the ultimate compressive strain attained in the concrete. This analytical formulation, representing the two non-linear stages of the cracked concrete section, will be approximated by a single relation described in the next section.

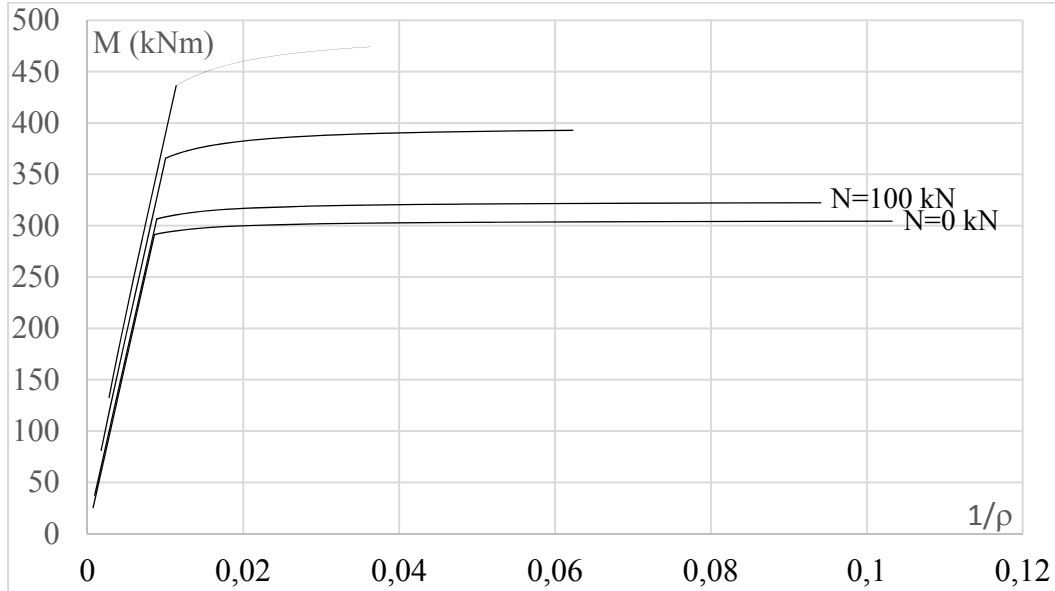


Figure 3: Analytical ( $M-I/\rho$ ) relationship for a particular case.

### 3.3 Stiffnesses considered at elastic and plastic steel

The equivalent elastic stiffness  $K_f$ , point 1 in Fig. 4, is considered to represent the last stage of cracked concrete with steel in the elastic range. This means that point 1 is the end of the steel in the elastic zone. Its value is the derivative of:

$$K_f = \left. \frac{dM}{d\rho} \right|_1 \quad (18)$$

The equivalent plastic stiffness  $K_p$  is computed at the point 2 with the corresponding bending moment,  $M_2$ , given by the derivative:

$$K_p = \left. \frac{dM}{d\rho} \right|_2 \quad (19)$$

The moment  $M_2$  corresponds to the maximum bending moment obtained for the ultimate limit state (conventional rupture for bending moment with or without axial force [20]). The moment  $M_0$  represented in Fig. 4, is established by:

$$M_0 = M_2 - K_p \frac{1}{\rho_2} \quad (20)$$

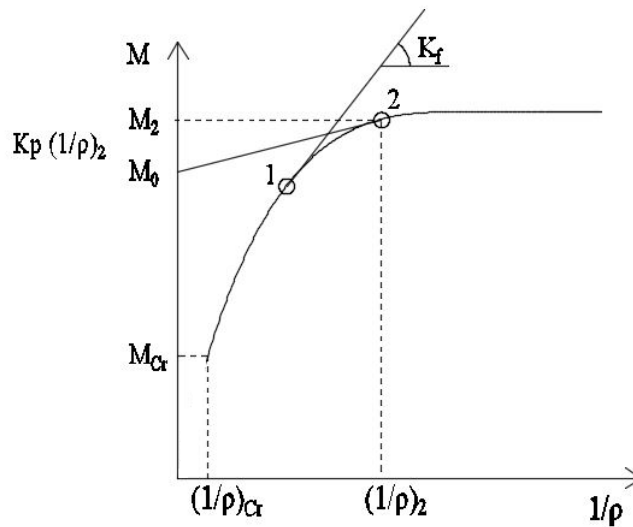


Figure 4: General moment-curvature diagram for cracked concrete.

#### 4 M-ρ OR ρ-M REPRESENTATIONS OF CRACKED SECTIONS

The representation of the moment curvature in a unique closed form can be obtained by two ways [2]: the curvature  $1/\rho$  in function of the moment  $M$  using the Ramberg - Osgood equation and the moment  $M$  in function of curvature  $1/\rho$  using the Goldberg Richard power representation. Both closed forms are described next.

##### 4.1 Ramberg - Osgood equation

A unique curvature- moment ( $1/\rho$ - $M$ ) relation, after the concrete cracking, denoted by state II, can be written using the Ramberg-Osgood equation as follows [2]:

$$\left[\frac{1}{\rho}\right]_2 = \frac{M}{K_f} + \alpha \frac{M}{K_f} \left(\frac{M}{M_0}\right)^{n-1} \quad (21)$$

In the last equation  $n$  is an integer number of the Ramberg-Osgood adjustment and  $\alpha$  is a parameter evaluated by:

$$\alpha = \frac{(K_f - K_p)}{K_p \left(\frac{M_2}{M_0}\right)^{n-1} n} \quad (22)$$

Fig. 5 compares the moment-curvature diagrams by Ramberg-Osgood equation with different values of the parameter  $n$  ( $n=6, 20, 40$ ) and the analytical curves for variable axial load applied in the particular section defined in the numerical results.

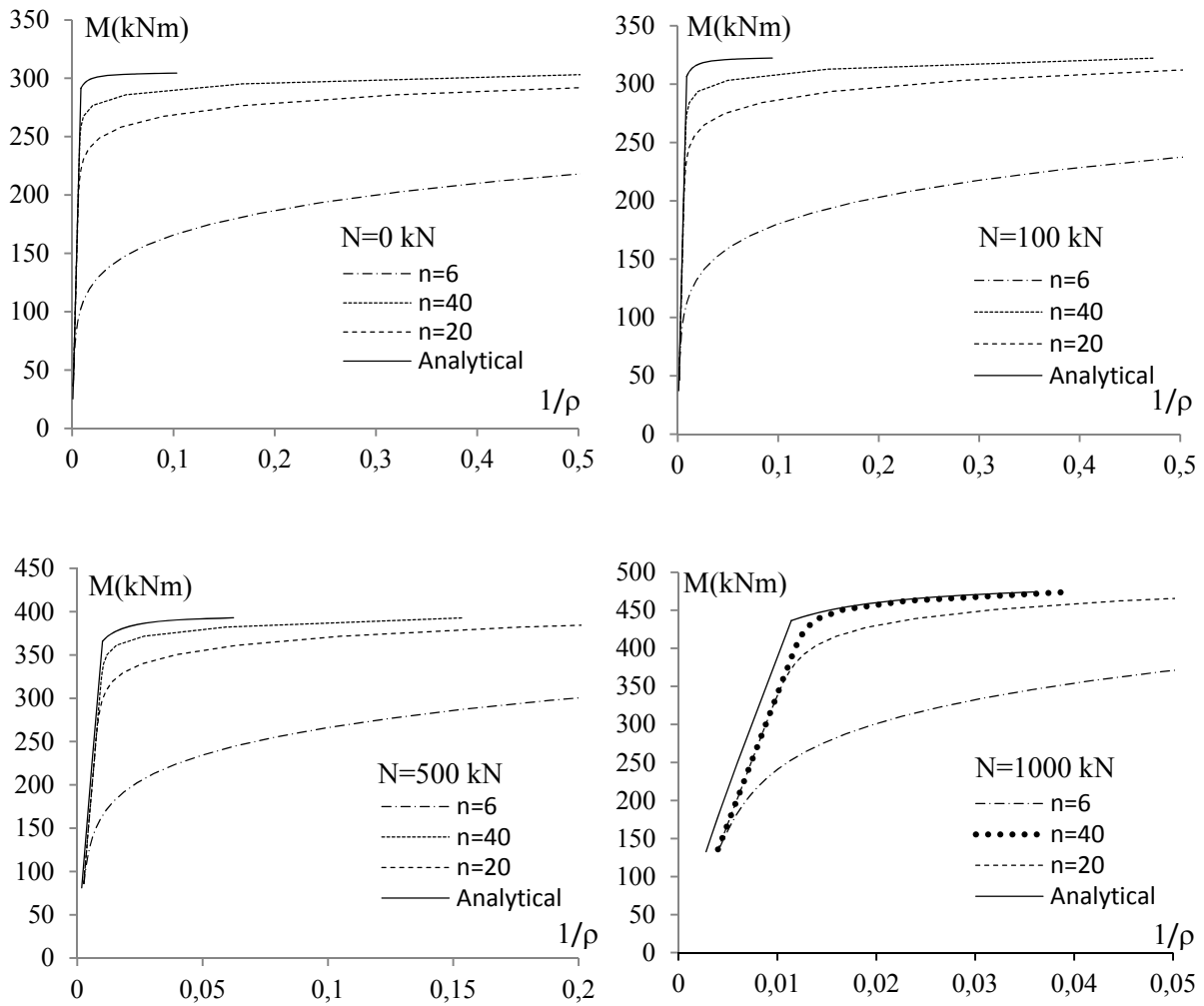


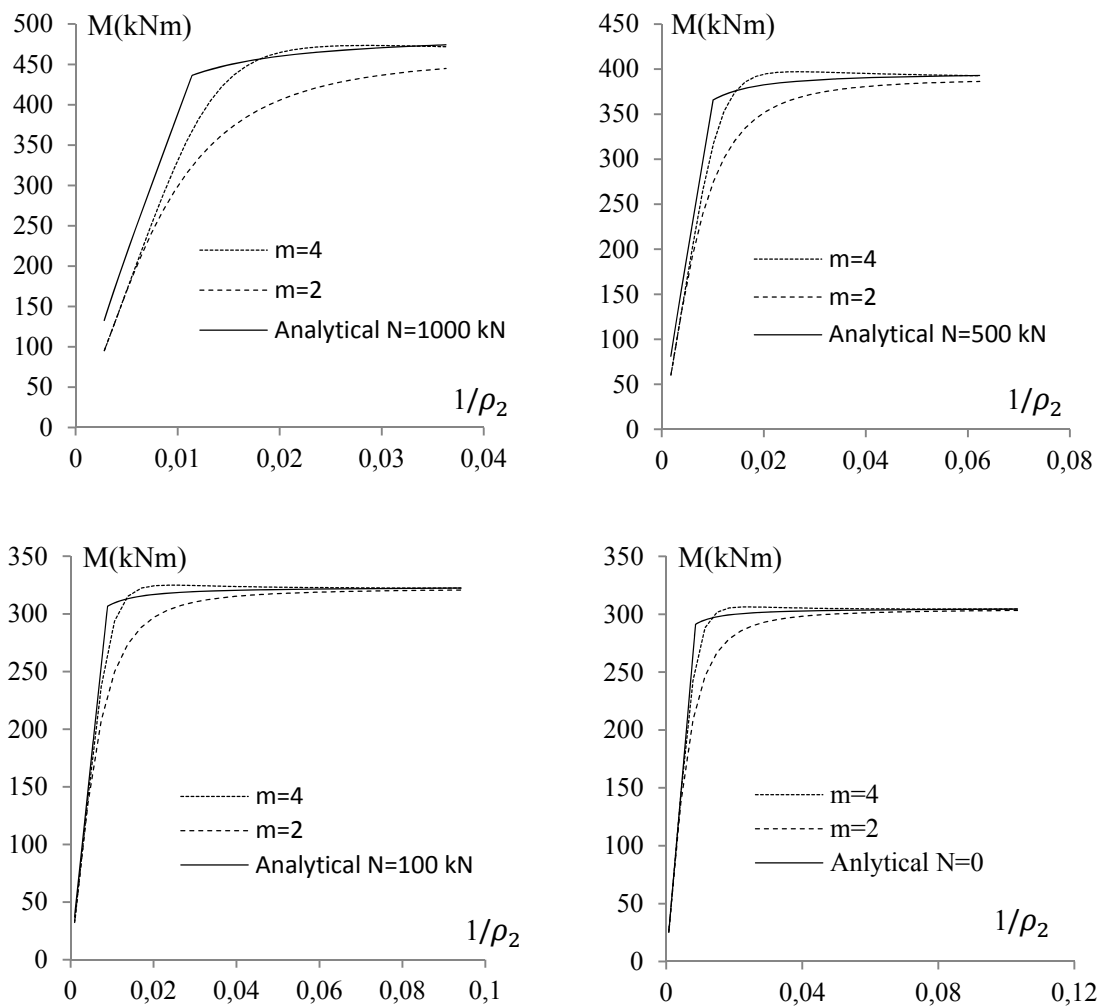
Figure 5: Moment-curvature diagram by Ramberg-Osgood equation.

#### 4.2 Goldberg Richard power representation

A closed form of the  $(M-1/\rho)$  relationship is obtained using the Goldberg Richard expression [2]. This equation gives the bending moment ( $M$ ) as a function of axial load ( $N$ ), the initial ( $K_f$ ) and the ultimate ( $K_p$ ) flexural stiffnesses:

$$M = \frac{(K_f - K_p)}{\rho \left( 1 + \left| \frac{(K_f - K_p) \frac{1}{\rho}}{M_0} \right|^m \right)^{1/m}} + K_p \frac{1}{\rho} \quad (23)$$

Fig. 6 represents this closed form applied to the same particular cases of Fig. 5.

Figure 6: Goldberg Richard power representation of  $(M-1/\rho_2)$ .

### 4.3 Comparison of the two representations

The previous moment-curvature approximation pointed out the need of the best parameters ( $n$  to Ramberg-Osgood, or  $m$  to Goldberg Richard equations) to employ in a particular case. Further, there is not a parameter  $n$ , for Ramberg-Osgood representation, satisfying simultaneously the moment and the corresponding curvature at the rupture for a wide range of loads in opposite to the choice of the  $m$  parameter in the Goldberg Richard equation. A comparison of the two representations is made in Fig. 7 for the same particular cases of Fig. 5, considering in the Ramberg-Osgood equation  $n=40$  and in the Goldberg-Richard  $m=4$ . In the figure, indicated as theoretical, is the analytical relationship composed by the equations for cracked concrete with elastic (equation (11)) and plastic steel (equation (17)). In this figure the uncracked concrete, for curvatures between 0 and  $(1/\rho)_{cr}$  and moments between 0 and  $M_{cr}$ , is not represented, that is, only the cracked concrete is approximated by the Ramberg-Osgood and Goldberg-Richard equations.

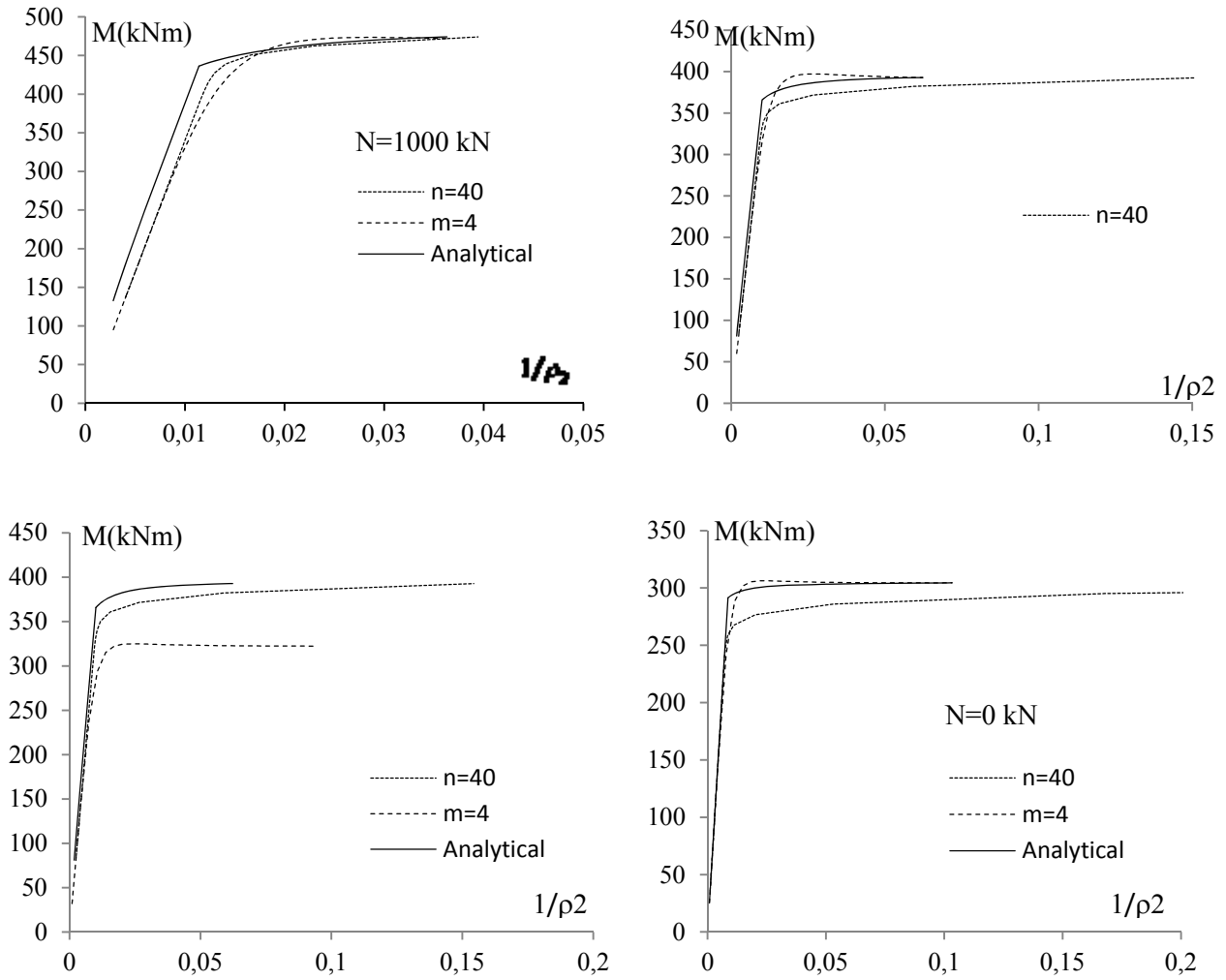


Figure 7: Comparison of the moment-curvature diagrams for cracked concrete.

The preference for the Ramberg-Osgood representation is due to the fact that the present model needs the curvature  $1/\rho$  as a function of the bending moment, in order to apply equation (1). It can be noted that the objective is to find a unique representation to the cracked stages,  $1/\rho_2$ , because the interaction used in (1) considers automatically the uncracked stage  $1/\rho_1$ .

## 5 NUMERICAL RESULTS

### 5.1 Moment curvature diagrams: Rectangular section under variable axial load

Figure 8 shows the moment curvature diagrams obtained for a rectangular symmetric reinforced cross section with variable axial load ( $N = 0, 100, 500, 1000kN$ ).

The cross section geometry is:  $b = 0,2m$ ;  $h = 0,4m$ ;  $a = 0,02m$ ;  $A_s = A_s' = 0,0021m^2$ . The material properties are :  $E_s = 200GPa$ ;  $E_c = 20GPa$ ;  $f_{yd} = 400MPa$ ;  $f_{ck} = 30MPa$  and  $f_{ctm} = 3MPa$ .

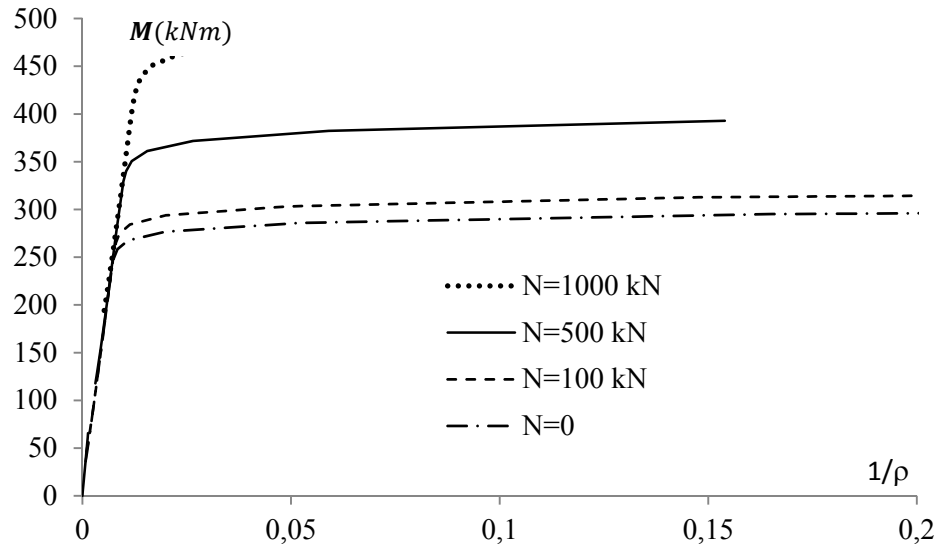


Figure 8: Moment- curvature diagrams of a RC section.

## 5.2 Moment curvature diagrams and deflection of a beam

The beam represented in Fig. 9a), is tested by Kwak et al [8]. The characteristics of the beam are the following:  $b=90\text{cm}$ ;  $d=27.23\text{cm}$ ;  $H=30.48\text{cm}$ ;  $B=15.24\text{cm}$ ;  $\rho'=0$ ;  $\rho=0.0062$ ;  $E_s=1.98 \times 10^6 \text{kg/cm}^2$ ;  $E_c=2.71 \times 10^5 \text{kg/cm}^2$ ;  $f_y=3236 \text{kg/cm}^2$ ;  $f_c=323 \text{kg/cm}^2$ . The mean concrete tensile strength used in the present analysis is:  $f_{ct} = f_c/10$ . Figure 9b) represents the moment curvature diagram considering: the Ramberg-Osgood equation with  $n=80$ ; the tension softening interaction given from equation 1 with the definition of  $\zeta$  by equation 2, considering  $\beta=1.0$  and  $0.5$ ; the results of Kwak et al [21] analysis made with 24 finite elements. Figure 9c) represents the load – central deflection diagram obtained with the model (for the two values of  $\beta$ ) and the experimental and analytical results of Kwak et al [21].

It can be observed in the figures that the present analytical model approximates the experimental results.

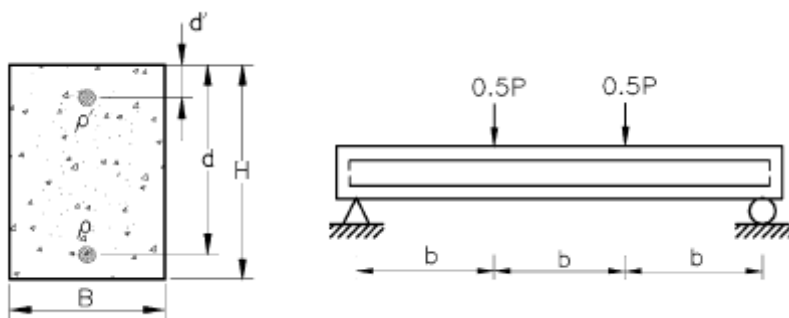


Figure 9a): Loading type and cross section of beam T1MA.

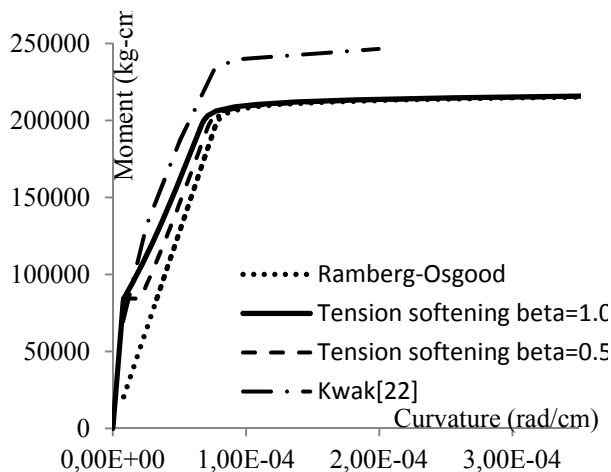


Figure 9b): Moment-curvature diagrams.

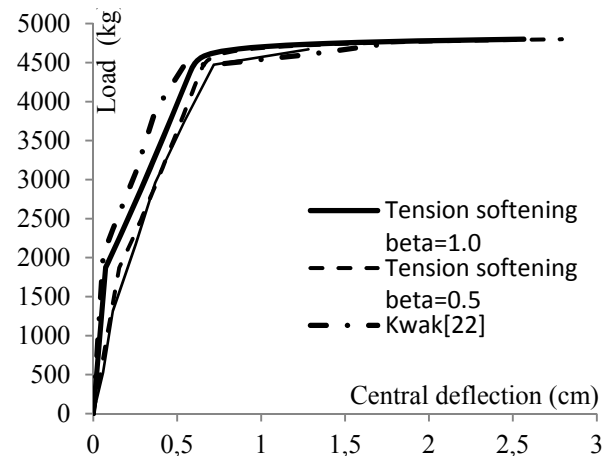


Figure 9c): Load deflection diagram.

## 6 CONCLUSIONS

The present work presents:

- the deduction of the moment curvature diagrams for singly or doubly reinforced concrete rectangular sections by MAPLE software with the three stages: *i*) uncracked concrete; *ii*) cracked concrete and steel in elastic domain; *iii*) cracked concrete and steel in plastic domain;
- the representation in a unique closed form of the curvature - moment relation using the Ramberg - Osgood equation. The moment – curvature equation with the Goldberg Richard power representation is also deduced and compared to the previous one;
- the analytical mean curvature of the structural member with the  $\zeta$  parameter of EC2;
- the deflection of the cracked member by the integration of the curvatures;
- the load – deflection curve of a RC beam and the comparison to other models and experimental results.

## ACKNOWLEDGEMENTS

This work has been supported by the Fundação para a Ciência e a Tecnologia (FCT) under project grant UID/MULTI/00308/2013.

## REFERENCES

- [1] Marques T., Ferreira, C. Barros H.; “Moment-curvature diagrams for reinforced concrete section design”, *2nd Int. Conf. on Numerical and Symbolic Computation Developments and Applications*, SYMCOMP 2015, Faro, 2015.
- [2] Faella, C., Piluso, V., Rizzano, G; *Strutural Steel Semirigid Connections – Theory, design and software*, CRC Press, 2000.
- [3] EN 1992-1-1; Eurocode 2 – *Design of concrete structures – Part 1-1: General rules and rules for buildings*, December, 2004.

- [4] Zheng H., Jinping O., Bo W., “The trilinear moment vs. curvature relationship of concrete beams reinforced with fiber reinforced polymer (FRP) rebars”, *Composite Structures*, 77, pp 30-35, 2007.
- [5] Torrico, F. A., *Theoretical and experimental analysis of slender high-strength concrete columns, considering the ductility*, PhD thesis, São Paulo University, Brazil, in Portuguese, 2009.
- [6] Challamel, N.; Hellesland, J.; “Buckling of softening columns in a continuum damage mechanics perspective – local versus non-local formulation”, *Journal of Mechanics and Solids*, 39, pp 229-242, 2013.
- [7] Ponaya, S.; Teeboonma, U.; Thinvongpituk, C.; “Plastic collapse analysis of thin-walled circular tubes subjected to bending”, *Thin Walled Structures*, 47, pp 637-645, 2009.
- [8] Vincent Picandet; Noel Challamel; Sovannara Hin; “Buckling and post-buckling of gradient and non-local plasticity columns experiencing softening”, *Int. Journal of Solids and Structures*, 51, pp 4052-4067, 2014.
- [9] Casandjian, C., Challamel, N, Lanos, C., Hellesland, J.; *Reinforced concrete beams, columns and frames: Mechanics and Design*, John Wiley& Sons, 2013.
- [10] Naci Caglar; Aydin Demir; Hakan Ozturk; Abdulhalim Akkaya; “A simple formulation for effective flexural stiffness of circular reinforced concrete columns”, *Eng. Applications of Artificial Intelligence*, 38, pp 79-87, 2015.
- [11] Cevik, A., Arslan, M. H., Koroglu, M. A., “Genetic-programming-based modelling of RC beam torsional strength”, *KSCE J. Civ. Eng.* 14 (3), pp 371-384, 2010.
- [12] Chen, H. M., Kao, W. K., Tsai, H. C., “Genetic-programming for predicting a aseismic abilities of school buildings”, *Eng. Appl. Artif. Intell.* 25 (6), pp 1103-1113, 2012.
- [13] *CEB Design Manual on Cracking and Deformation*, CEB, 1985.